




Water Adsorption Thermodynamical Analysis and Mechanical Characterization of Chitosan and Polyvinyl Alcohol-Based Films

Rocio Y. Aguirre-Loredo¹ · Gonzalo Velazquez² · Andrea Y. Guadarrama-Lezama³  · Rubi Viveros-Contreras⁴ · Johanna Castaño⁵

Accepted: 14 October 2021 / Published online: 1 November 2021

© The Author(s), under exclusive licence to Springer Science+Business Media, LLC, part of Springer Nature 2021

Abstract

Chitosan and polyvinyl alcohol films were prepared by the casting method. Moisture adsorption isotherms were obtained at 15 °C, 20 °C, 25 °C and 30 °C. Experimental isotherms were well fitted using the GAB model ($E < 10\%$). The thermodynamic analysis showed a minimum integral entropy (ΔS_{int}) at the 0.3–0.6 range of water activity (a_w) in all films. Pore radius values of the films ranged from 1.005 nm to 20.766 nm, which correspond to the micropores and mesopores classification. Compensation enthalpy-entropy in films showed that the water vapor adsorption process was driven by enthalpy at low a_w values (0.3–0.5 for CS and 0.2–0.3 for PVA). Most of the mechanical properties showed constant values at the zone of minimum ΔS_{int} , confirming that thermodynamic properties could be used to predict the stability of films. The study of thermodynamic water adsorption and the mechanical properties allows understanding the preparation process of stable films with adequate parameters intended for food packaging materials.

Keywords Chitosan · Polyvinyl alcohol · Films · Thermodynamic properties · Mechanical properties

Introduction

The use of packaging materials based on synthetic polymers has been reduced in many countries due to environmental concerns. Packaging should be able to protect foods keeping

their physicochemical characteristics, where controlling the moisture transfer is an important factor. Because most food products are stored in humid environments, it is essential to know the behavior of films under several conditions. For this reason, the replacement of synthetic materials by biodegradable materials must be evaluated in terms of its physical, mechanical, and moisture adsorption properties in order to predict the performance as a food packaging material.

Among the polymers used to prepare films are chitosan (CS) and polyvinyl alcohol (PVA). Chitosan consists of N-acetyl-D-glucosamine and D-glucosamine units linked by (1–4) bonds [1]. It has excellent film-forming ability allowing obtaining biodegradable materials with moderate water vapor barrier, adequate mechanical properties, and low oxygen permeability [2]. Because of its composition, chitosan films can adsorb a high amount of water even when pure chitosan is only soluble in 1% acid solutions. Some advantages of using chitosan as a film-forming polymer include the high compatibility with other biopolymers to form homogeneous structures because of its chemical composition. CS is a natural cationic copolymer with abundant water-binding groups and is soluble in weakly acidic aqueous solutions. This polymer contains hydroxyl, carbonyl, amino- and acetamide groups, that can adsorb a high amount of water [3–5].

✉ Andrea Y. Guadarrama-Lezama
ayguadarramal@uaemex.mx

✉ Rubi Viveros-Contreras
ruviveros@uv.mx

¹ Departamento de Procesos de Polimerización, CONACYT-CIQA, Blvd. Enrique Reyna Hermosillo 140, Saltillo, Coahuila 25294, México

² CICATA, Unidad Querétaro, Instituto Politécnico Nacional, Cerro Blanco 141, Colinas del Cimatario, CP 76090 Santiago de Querétaro, México

³ Facultad de Química, Universidad Autónoma del Estado de México, Paseo Colón Esq. Paseo Toluca S/N, Col. Residencial Colón, CP 50120 Toluca, Estado de México, México

⁴ Centro de Investigaciones Biomédicas, Universidad Veracruzana, Doctor Castelazo Ayala S/N, Industrial Animas, 91190 Xalapa Enríquez, Veracruz, México

⁵ Facultad de Ingeniería y Tecnología, Universidad San Sebastián, Lientur 1457, 4080871 Concepción, Chile

PVA has been considered as a truly biodegradable material because of its excellent hydrophilicity and biocompatibility [6–8]. These properties have led to the use of PVA in a wide range of applications in medical, cosmetic, food, pharmaceutical, and packaging industries. Also, it has an excellent capability to form films with good flexibility, tensile strength, and barrier properties to gas and vapor [9].

PVA films are extensively used in food packaging and several applications as reinforcing material when mixed with compatible biopolymers. The main properties of PVA depend on the acetate and hydroxyl groups present in its chemical structure [10]. PVA and chitosan polymers have been used alone or in mixtures with other polymers as film formers, but the relationship among moisture adsorption, mechanical, and thermodynamic properties has not been totally evaluated [1, 11–16].

Knowing the water adsorption capacity of materials allows deciding the best application as this property influences the stability and quality changes in packed foods. Also, it helps to predict the performance of the films under different relative humidity conditions. Obtaining the equilibrium moisture content allows estimating the moisture adsorption isotherms, which is necessary to predict the hydrophilic-hydrophobic properties of the films. The moisture content in polymers influences their stability and hydration, among other properties that are related to their performance under real application conditions.

Enthalpy and entropy are thermodynamic parameters used to identify the mechanism and the energy requirements of the adsorption process. Based on that, the purpose of this study is to gain knowledge about the moisture adsorption properties of a synthetic (PVA) and a natural (CS) film-forming polymer.

The research work was carried out in four stages: (1) to determine the moisture adsorption isotherms of CS or PVA based films, (2) to assess the thermodynamic properties to describe the stability conditions for storage of the films, (3) to describe the mechanism of water vapor adsorption through compensation enthalpy-entropy theory, (4) to correlate the thermodynamic and mechanical properties in order to describe its stability.

Materials and Methods

Materials

Chitosan from shrimp shell was purchased from Sigma–Aldrich (USA, degree of deacetylation > 75 %). Polyvinyl alcohol with a 99.0–99.8 % degree of hydrolysis was purchased from J.T. Baker (USA). Glacial acetic acid was purchased from Fermont, Mexico. LiCl, MgCl₂, K₂CO₃·2H₂O, KCl, NaCl, NaBr, and BaCl₂·2H₂O (Jalmek

Científica, Monterrey, México) were used for the moisture adsorption isotherms. All salts were reagent grade with at least 99 % purity.

Methods

Films Preparation

Films from CS were prepared following the procedure described by [11]. Briefly, the chitosan (1 g) was dissolved in 100 ml of 1% (v/v) acetic acid solution, stirred for two hours and then centrifuged at 3000 rpm (Eppendorf, model 580HR) for 20 min to remove air bubbles and insolubilized particles. The films were prepared using the casting method, pouring 100 ml of the filmogenic solution into glass molds (150 × 150 mm). The solution was dehydrated under forced convection (Excalibur Dehydrator, Sacramento, CA. Model 3962 T) at 35 ± 1 °C for 3 h at 1 ms⁻¹ air-flow. After drying, the films were peeled, placed in plastic bags inside a desiccator with silica gel, and stored at room temperature. Films from PVA were prepared according to the method reported by [14]. Briefly, the film-forming solution was prepared with 2% (w/v) of PVA, heating at 70 °C while stirring for 1 h. The air bubbles formed in the filmogenic solution were removed using a vacuum pump (Buchi V700, Germany). Then, the solution (100 ml) was cast into a 150 × 150 mm glass mold and dried in a forced convection dehydrator (Excalibur Dehydrator, Sacramento, CA. Model 3962 T) at 50 °C for 3 h at 1 ms⁻¹ airflow. After drying, films were also stored at room temperature in plastic bags inside a desiccator with silica gel.

Moisture Adsorption Isotherms

For the moisture adsorption isotherms, the films were equilibrated in a desiccator containing silica gel for 1 week to maintain the RHeq as close as possible to zero (RHeq = 3%) and the adsorption isotherms were obtained following the gravimetric method reported by McCune et al. [17]. Film samples (60 × 15 mm) were placed into wide-mouth air-tight acrylic vessels containing oversaturated solutions of different salts that supplied equilibrium relative humidity values from 11 to 90%, equivalent to water activity (a_w) values in the 0.11–0.90 interval [18]. To allow the adsorption of moisture, the films were placed on a plastic mesh allocated above the saturated salt solutions on a perforated plate. Five vessels with different HReq for each sample were placed in a forced convection chamber controlled at 15 °C, 20 °C, 25 °C, or 30 °C (± 0.1). At each temperature, the experiments were conducted in triplicate. After reaching equilibrium (about 10 days), the

films were weighed (Ohaus balance model AP210, Pine Brook, NJ, USA) and the moisture content was determined gravimetrically after drying (Felisa model FE 100, Mexico City, Mexico) at 110 °C for 20 h. Moisture adsorption isotherms were fitted to the Guggenheim-Anderson-De Boer (GAB) model (Eq. 1) by non-linear regression using Kaleida Graph from Synergy software (Reading PA, USA).

$$M = \frac{M_0CKa_w}{(1 - Ka_w)(1 - Ka_w + CKa_w)} \quad (1)$$

where M is the equilibrium moisture content (g H₂O/100 g of dry solids (d.s.)), M_0 is the moisture content in the monolayer (g H₂O /100 g d.s.), C is the Guggenheim constant, and K is the constant correcting the properties of the multilayer molecules with respect to the bulk liquid. To assess the accuracy of the fitting, the relative percentage difference (E) was used. It is generally assumed that values of $E < 10\%$ indicate a good fit.

Sorption Properties of Films

Determination of Pore Radio

The sorption area on the solid surface determines the water binding capacity of the materials and it is calculated from the monolayer moisture content (M_0) using Eq. 2 [19, 20].

$$S_0 = M_0 \frac{1}{M_w} N_0 A_{H_2O} = 3.5 \times 10^3 M_0 \quad (2)$$

where M_w is the water molecular weight (kg/mol), N_0 is the Avogadro number (6.0×10^{23} molecules/mol), and A_{H_2O} denotes the water molecule area (1.06×10^{-19} m²). The pore radius is useful when studying the adsorption phenomenon [21]. The critical pore radius was determined by the Kelvin expression described by Eq. 3.

$$r_c = -\frac{2\sigma V_M}{RT \ln(a_w)} \quad (3)$$

Here, r_c is the critical radius (m), R is the universal gas constant (8.314×10^{-3} kJ/mol K), V_M is the molar volume of sorbate (m³/mol), σ is the surface tension (N/m), and T is the temperature in °K. Besides, the Halsey equation was used to estimate the adsorbed water multilayer thickness (t) [20, 22] as expressed by Eq. 4.

$$t = 0.354 \left(\frac{-5}{\ln a_w} \right)^{1/3} \quad (4)$$

$$H_V^0(T) \text{ J/mol}^{-1} \text{K}^{-1} = 6.15 \times 10^4 - 94.14T + 17.74 \times 10^{-2}T^2 - 2.03 \times 10^{-4}T^3 \quad (10)$$

The sum of the multilayer thickness and the critical radius (Eq. 5) was considered as the pore radius (r_p) [23, 24].

$$r_p = r_c + t \quad (5)$$

Thermodynamic Properties

The physical stability of the films was evaluated through the enthalpy and entropy parameters. The changes of the integral enthalpy (ΔH_{int})_T (kJ/mol) at the different water activities were calculated using the model of Othmer [25] (Eq. 6).

$$\frac{\partial \ln P_V}{\partial \ln P_V^0(T)} = \frac{H_V(T)}{H_V^0(T)} \quad (6)$$

where: P_V (atm) is the water vapor pressure in the sample, $H_V(T)$ (kJ/mol) is the integral molar heat of adsorption, $P_V^0(T)$ (atm) is the vapour pressure (atm) of pure water at the temperature of adsorption, and $H_V^0(T)$ (kJ/mol) is the condensation heat of pure water. As all terms depend on the temperature, the Eq. 6 can be integrated as follows:

$$\ln P_V = \left[\frac{H_V(T)}{H_V^0(T)} \right]_{\phi} \ln P_V^0 + A \quad (7)$$

where ϕ (kJ/mol) is the surface potential or diffusion pressure and A is the adsorption constant. A straight line is obtained in a plot of $\ln P_V$ versus $\ln P_V^0(T)$ when the ratio $H_V(T)/H_V^0(T)$ is constant in the temperature range studied.

At the same pressure of diffusion for each isotherm, the molar integral enthalpy (ΔH_{int})_T was calculated using Eq. (8) [26].

$$(\Delta H_{int})_T = \left[\frac{H_V(T)}{H_V^0(T)} - 1 \right]_{\phi} H_V^0(T) \quad (8)$$

$$\phi = \mu_{ap} - \mu_a = RT \frac{W_{ap}}{W_v} \int_0^{a_w} M d \ln(a_w) \quad (9)$$

where μ_{ap} and μ_a (kJ/mol) are the chemical potential of the adsorbent pure and of the condensed phase, respectively, meanwhile W_{ap} and W_v (kg/mol) are the molecular weight of the adsorbent and the water, respectively.

The integral enthalpy at different temperatures was obtained after calculating $H_V(T)/H_V^0(T)$ from Eq. (7) and substituting it into Eq. (8) using the estimation of $H_V^0(T)$ proposed by Wexler [27]:

From the values of $(\Delta H_{int})_T$, the changes in the integral molar entropy $(\Delta S_{int})_T$ were calculated using Eq. (11).

$$(\Delta S_{int})_T = S_s - S_L = -\frac{(\Delta H_{int})_T}{T} - R \ln a_w \quad (11)$$

where S_L (kJ/mol K) is the molar entropy of liquid water in equilibrium with vapor; $S_s = S/N_l$ (kJ/mol K) is the integral entropy of the water adsorbed. In this last expression, S (kJ/mol K) is the total entropy of the adsorbed water and N_l is the moles of adsorbed water.

Compensation Theory

The enthalpy-entropy compensation theory assumes that there is a linear relationship between enthalpy and entropy. The ΔH_{int} and ΔS_{int} values are correlated in the compensation law (Eq. 12).

$$\Delta H_{int} = -T_\beta \Delta S_{int} + \Delta G_\beta \quad (12)$$

where T_β is the isokinetic temperature at which all reactions take place at an equal rate; ΔS_{int} is the integral entropy; ΔG_β is the free energy at the isokinetic temperature. When $\Delta G_\beta < 0$, the sorption of water is occurring spontaneously.

The comparison of T_β (isokinetic temperature) with the harmonic mean temperature (T_{hm}), defined by Eq. (13), is used to corroborate the compensation theory [28].

$$T_{hm} = \frac{N}{\sum_{i=1}^N (1/T)} \quad (13)$$

The compensation theory can be applied only when $T_\beta \neq T_{hm}$.

Mechanical Properties of Films

The maximum stress (GPa) and the Hencky strain at the breaking of the films were assessed at room temperature (25 °C) in CS and PVA films conditioned at several RHeq values following the specifications of the ASTM D882-12 [29]. Film samples (10 × 100 mm) were cut and conditioned in microclimates from 11 to 90 % RHeq for 7 days at 30 °C in the same saturated saline solutions used to determine the moisture adsorption isotherm. A texture analyzer (TA Plus, Lloyd Instruments, UK) was used to measure the mechanical properties. The initial separation of the mechanical grips was set at 50 mm and a crosshead speed of 1 mm/s was used for the test. Fifteen replicates were analyzed for each film and only the samples broken at the middle point were considered. The average thickness was 0.0381 ± 0.0079 mm and 0.0403 ± 0.0089 mm for CS and PVA films, respectively.

Toughness, defined as the energy per unit of volume absorbed by a material before rupturing [15], was calculated as the area under the stress—strain curve per volume of the film sample [1].

$$T = \frac{E}{V} = \int_0^{\epsilon_f} \sigma d\epsilon \quad (14)$$

where E means energy; V is the volume; σ is the stress; ϵ is Hencky strain (HS); and ϵ_f is the Hencky strain value at the film breaking.

Statistical Analysis

The results were presented as mean values \pm SD (standard deviation). One-way ANOVA was carried out using the Minitab software (Minitab Inc., State College, PA, USA). To determine the statistically significant difference between means, the Tukey's test ($p \leq 0.05$) was applied.

The coefficient of determination (R^2) and the mean relative deviation modulus (E) given by Eq. 15 were used to assess the fitting of the GAB model to the moisture adsorption isotherm.

$$E = \frac{100}{n} \sum \left| \frac{M_i - M_{Ei}}{M_i} \right| \quad (15)$$

where M_i is the i th moisture content, M_{Ei} is the estimated moisture content and n is the number of experimental points. Values of $E < 10\%$ indicate an acceptable fit.

Results and Discussion

Moisture Adsorption Isotherms

Figure 1 shows the experimental and fitted moisture adsorption isotherms of CS and PVA films at 15 °C, 20 °C, 25 °C, and 30 °C. Films from CS were more hygroscopic, whereas the PVA films presented the lowest equilibrium moisture contents. At a constant a_w value, the amount of adsorbed moisture decreased as the temperature increased. This phenomenon was more evidenced in CS films. This behavior could be explained by the chemical structure and availability of the hydrophilic regions of each polymer to bind water.

The moisture content of CS films at 0.75 a_w was approximately two folds higher than that of PVA films, indicating that the former was more hydrophilic. The greater moisture content for CS can be attributed to the formation of a rigid structure, characterized by numerous hydrogen bonds. Water adsorption isotherm evidenced that the PVA and CS films adsorb $< 20\%$ moisture when exposed to high relative

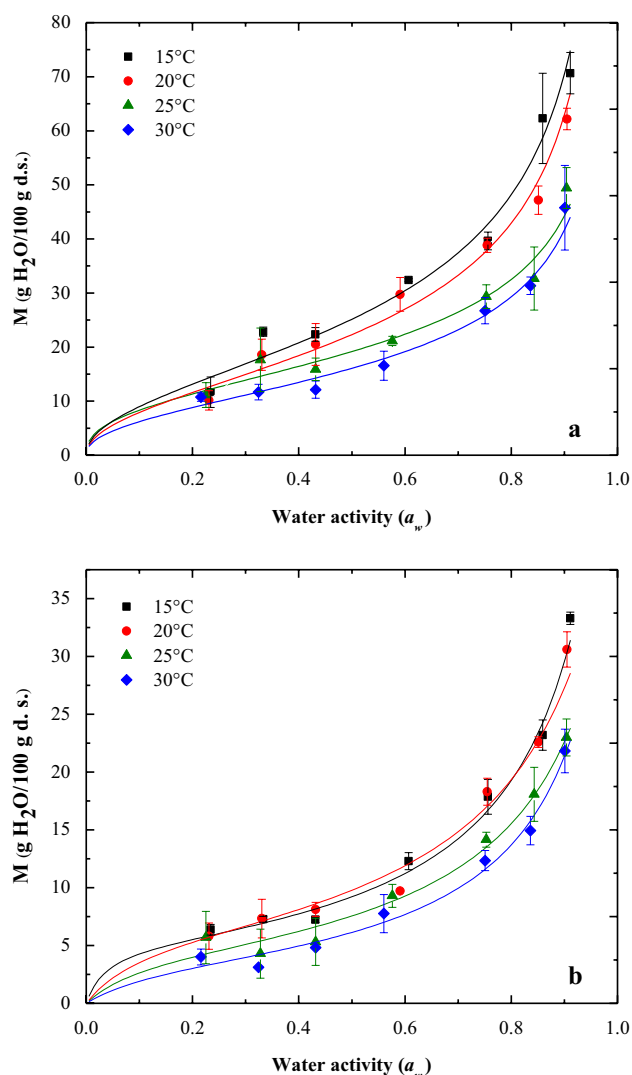


Fig. 1 Moisture adsorption isotherms on **a** Chitosan and **b** PVA films. Symbols (Red filled circle, Black filled cube, green filled triangle, blue filled diamond) correspond to the experimental results and continuous lines to fitted ones by using the GAB equation

humidity ambient conditions similar to the results reported by Aguirre-Loredo et al. [11].

The CS and PVA isotherms had a typical type II sigmoid shape. In this type of isotherms, the affinity of adsorbate by adsorbent is slightly high than the affinity by the adsorbent itself [30]. This adsorption behavior leads to the formation of monolayer and multilayers [31]. In the monolayer region, the moisture content of the films did not show important changes as a_w increased, indicating a stability region [32]. From this point of view, the less water affinity in PVA films in comparison with CS films could help to decide its application as semi-impermeable packaging material.

The experimental moisture adsorption data were well fitted to the GAB equation. Table 1 summarizes the values

for M_0 , C , and K calculated from the GAB equation at the temperatures studied for PVA and CS films. The coefficients of determination (R^2) were higher than 0.990 and E values were $\leq 10\%$, indicating a good fit [33]. The monolayer (M_0) moisture content shows the amount of water strongly adsorbed at specific binding sites in the material and it is considered as the optimum moisture content to reach the maximum stability of the polymeric material [34]. Increasing the temperature from 15 to 30 °C in CS and PVA films, resulted in a decrease in the M_0 values. The M_0 values for PVA films were lower than those of CS films for all temperatures. Since adsorption is a physical phenomenon, this behavior is attributed to a reduction in the number of available sites for water binding due to an increase in the kinetic energy of the water molecules and the functional groups of the binding sites promoting the distance apart. Water molecules with a low vibration are more easily bound to binding sites on the polymeric chain [35]. The chemical structure of CS and PVA is also involved as CS has a higher number of hydroxyl groups available to bind water molecules by electrostatic interactions [36]. On the other hand, the acetate groups in the PVA_{99%} are bulkier than hydroxyl groups making more difficult the packaging of PVA macromolecules resulting in a decrease of water adsorption.

The C parameter in the GAB model is related to the adsorption energy of water molecules to primary active sites [37]. In this work, the values of C for films ranged from 7.54 to 278.96 Table 1 and they did not show a trend with temperature. Usually, high C values have no physical meaning as they are a result of a mathematical fitting, which usually occurs when using models with three or more parameters [38–40].

The K parameter assumes that the water molecules in the multilayer interact with the sorbent changing the adsorption energy levels to values between the monolayer and the free water molecules. Usually, the K value is lower than 1 [34]. The K values close to 1 indicate a reduction of the adsorption energy which suggests a disruption of the multilayer to a bulk liquid-like domain [41]. In this work, K values for all films ranged from 0.818 to 0.919, indicating a better structured state of the water molecules in the layer adjacent to monolayer of films.

Sorption Properties of Films

The radio pore and surface area influence the sorption properties of the materials. The surface area of sorption for CS and PVA films is shown in Table 2. The surface area values decreased as the temperature increased as a consequence of a reduction in the available sites of sorption, and also because of the decreasing in the binding sorption energy associated with the monolayer and multilayer [39].

Table 1 Estimated parameters of the GAB equation for CS and PVA films

Film	Temperature °C	M_0 (g H ₂ O/100 g of dry solid)	C	K	R^2	E (%)
Chitosan (CS)	15	16.339 ± 0.20 ^a	10.874 ± 0.05 ^a	0.853 ± 0.10 ^a	0.989	9.661
	20	16.265 ± 0.10 ^a	7.540 ± 0.02 ^b	0.818 ± 0.12 ^a	0.991	8.380
	25	10.434 ± 0.30 ^b	278.96 ± 0.06 ^c	0.871 ± 0.06 ^a	0.992	8.901
	30	8.600 ± 0.15 ^c	97.265 ± 0.03 ^d	0.876 ± 0.05 ^a	0.992	5.510
Polyvinyl alcohol (PVA)	15	6.196 ± 0.35 ^a	11.388 ± 0.11 ^a	0.865 ± 0.13 ^a	0.993	7.311
	20	5.197 ± 0.20 ^b	29.094 ± 0.15 ^b	0.917 ± 0.05 ^a	0.994	4.920
	25	4.718 ± 0.10 ^c	10.671 ± 0.13 ^c	0.885 ± 0.12 ^a	0.990	10.101
	30	3.790 ± 0.12 ^d	8.337 ± 0.17 ^d	0.919 ± 0.05 ^a	0.992	10.080

^aCS Chitosan, PVA Polyvinyl alcohol, M_0 Moisture content of the monolayer (g water/100 g d.s.), C and K GAB model constants, a_w Water activity, R^2 Coefficient of linear determination, E Mean relative deviation modulus (%)

^bResults are presented as means ± SD ($n=3$)

^cValues with different letters in the same column indicate significant difference ($p \leq 0.05$)

Table 2 Surface area of sorption (m²/g) for CS and PVA films

Films	15 °C	20 °C	25 °C	30 °C
CS	579.231 ± 21.70 ^a	576.610 ± 19.90 ^a	369.890 ± 20.05 ^b	304.871 ± 19.90 ^c
PVA	219.660 ± 10.02 ^a	184.231 ± 9.21 ^b	167.251 ± 7.43 ^c	134.350 ± 7.72 ^d

^aCS Chitosan, PVA Polyvinyl alcohol

^bResults are presented as means ± SD ($n=3$)

^cValues with different letters in the same row indicate significant difference ($p \leq 0.05$)

The CS films had the highest values of surface area Table 2. It could be related to the availability of polar groups on the surface of CS films to catch water molecules because this polymer is composed mainly of hydroxyl groups [36]. As a result of the hydrophilic interaction, the water molecules could be bound by hydrogen forces at the tested temperatures. From these results, it can be assumed that the solid surface area of sorption is influenced by differences in the chemical composition of the absorbate.

The microporous properties determine the adsorption potential in solid materials [42]. Table 3 shows the pore radio (r_p) values for CS and PVA films, which ranged from 0.816 nm to 13.44 nm for the different moisture contents. In general, the pore radio values increased as the temperature and moisture content increased, being PVA films those having the highest values. According to the radio values, it is possible to classify the porous as micropores (<2 nm) or mesoporous (2–50 nm) [39]. The presence of mesopores prevails in a wider range of moisture content for CS and PVA films. At lower moisture content (20–22 g H₂O/100 g d.s.), at 15 °C and 20 °C, the CS films presented micropores, while at the highest moisture contents (23–30 g H₂O/100 g d.s.), the films were in the mesopore classification.

As the temperature increased (25 °C and 30 °C) micropores in films were present at lower moisture content (15–18 g H₂O/100 g d.s.) compared with 15 °C and 20 °C. A similar

behavior was observed in PVA films, but the micropores (0.8–1.87 nm) were present in a narrower moisture content (<10 g H₂O/100 g d.s.) compared to CS films, in the range of the studied temperatures (15 °C to 30 °C).

The differences in pore radio and water sorption for CS and PVA can be attributed to the chemical composition of biopolymers and their molecular structure. According to Mucha & Ludwiczak [43], the acetamide group in the chitin, an important component of chitosan, imposes steric limitations hindering the packing of the structure. It is in line with the stated by Ogawa et al. [44], who mentioned that chitosan adopts three-dimensional conformations in compact and extended structures as a function of the water content (hydrated or anhydrous) adopting spontaneous conformations. The voids in the polymeric matrix can be filled with water molecules. As described by Rivero [45], water acts as a plasticizer in chitosan, influencing its molecular packaging properties. The adsorbed water molecules increase the separation between polymeric chains (unpackaging), influencing the hole radio (pore radio). Okuyama et al. [46] evidenced that water molecules form columns between sheets of chitosan and contribute to stabilize the structure by making water-bridges between the polymer chains. It seems like those conformations of chitosan in presence of water influence the packaging or unpackaging leading to the formation of micropores or mesoporous in presence of water.

Table 3 Pore radius (nm) at different moisture contents and temperatures for CS and PVA films

Moisture content (g H ₂ O/100 g d.s)	CS films				Moisture content (g H ₂ O/100 g d.s)	PVA films			
	15 °C	20 °C	25 °C	30 °C		15 °C	20 °C	25 °C	30 °C
10	1.005 ± 0.01 ^a	1.073 ± 0.01 ^b	1.061 ± 0.05 ^c	1.293 ± 0.06 ^d	10	2.331 ± 0.05 ^a	2.459 ± 0.02 ^b	3.072 ± 0.04 ^c	3.728 ± 0.03 ^d
11	1.065 ± 0.04 ^a	1.144 ± 0.04 ^b	1.145 ± 0.06 ^c	1.407 ± 0.01 ^d	11	2.621 ± 0.06 ^a	2.770 ± 0.03 ^b	3.467 ± 0.05 ^c	4.183 ± 0.06 ^d
12	1.128 ± 0.02 ^a	1.218 ± 0.06 ^b	1.237 ± 0.07 ^c	1.532 ± 0.02 ^d	12	2.933 ± 0.03 ^a	3.093 ± 0.06 ^b	3.892 ± 0.06 ^c	4.665 ± 0.07 ^d
13	1.194 ± 0.03 ^a	1.296 ± 0.05 ^b	1.339 ± 0.01 ^c	1.667 ± 0.04 ^d	13	3.266 ± 0.02 ^a	3.430 ± 0.04 ^b	4.350 ± 0.06 ^c	5.176 ± 0.08 ^d
14	1.264 ± 0.05 ^a	1.379 ± 0.08 ^b	1.450 ± 0.04 ^c	1.814 ± 0.03 ^d	14	3.623 ± 0.05 ^a	3.779 ± 0.07 ^b	4.844 ± 0.07 ^c	5.718 ± 0.09 ^d
15	1.337 ± 0.02 ^a	1.466 ± 0.03 ^b	1.572 ± 0.02 ^c	1.972 ± 0.05 ^d	15	4.004 ± 0.02 ^a	4.141 ± 0.06 ^b	5.378 ± 0.02 ^c	6.295 ± 0.04 ^d
16	1.414 ± 0.06 ^a	1.558 ± 0.01 ^b	1.703 ± 0.03 ^c	2.142 ± 0.03 ^d	16	4.409 ± 0.01 ^a	4.515 ± 0.04 ^b	5.954 ± 0.04 ^c	6.908 ± 0.09 ^d
17	1.494 ± 0.01 ^a	1.654 ± 0.02 ^b	1.846 ± 0.02 ^c	2.324 ± 0.04 ^d	17	4.841 ± 0.04 ^a	4.901 ± 0.03 ^b	6.576 ± 0.03 ^c	7.561 ± 0.08 ^d
18	1.577 ± 0.03 ^a	1.754 ± 0.07 ^b	1.999 ± 0.01 ^c	2.517 ± 0.05 ^d	18	5.299 ± 0.04 ^a	5.300 ± 0.08 ^b	7.247 ± 0.02 ^c	8.255 ± 0.03 ^d
19	1.664 ± 0.08 ^a	1.859 ± 0.05 ^b	2.164 ± 0.02 ^c	2.722 ± 0.07 ^d	19	5.784 ± 0.02 ^a	5.712 ± 0.02 ^b	7.971 ± 0.03 ^c	8.993 ± 0.01 ^d
20	1.755 ± 0.02 ^a	1.968 ± 0.03 ^b	2.341 ± 0.03 ^c	2.940 ± 0.05 ^d	20	6.299 ± 0.06 ^a	6.136 ± 0.10 ^b	8.750 ± 0.09 ^c	9.779 ± 0.05 ^d
21	1.849 ± 0.04 ^a	2.082 ± 0.04 ^b	2.530 ± 0.01 ^c	3.170 ± 0.08 ^d	21	6.842 ± 0.07 ^a	6.572 ± 0.07 ^b	9.588 ± 0.01 ^c	10.614 ± 0.06 ^d
22	1.947 ± 0.06 ^a	2.201 ± 0.04 ^b	2.732 ± 0.06 ^c	3.413 ± 0.06 ^d	22	7.417 ± 0.01 ^a	7.020 ± 0.05 ^b	10.487 ± 0.02 ^c	11.500 ± 0.04 ^d
23	2.049 ± 0.03 ^a	2.324 ± 0.09 ^b	2.946 ± 0.05 ^c	3.668 ± 0.05 ^d	23	8.022 ± 0.01 ^a	7.481 ± 0.08 ^b	11.452 ± 0.03 ^c	12.441 ± 0.03 ^d
24	2.154 ± 0.08 ^a	2.452 ± 0.01 ^b	3.174 ± 0.02 ^c	3.936 ± 0.08 ^d	24	8.660 ± 0.04 ^a	7.953 ± 0.01 ^b	12.485 ± 0.07 ^c	13.439 ± 0.05 ^d
25	2.263 ± 0.03 ^a	2.585 ± 0.03 ^b	3.415 ± 0.05 ^c	4.217 ± 0.07 ^d	25	9.330 ± 0.03 ^a	8.438 ± 0.04 ^b	13.590 ± 0.09 ^c	14.497 ± 0.08 ^d
26	2.376 ± 0.04 ^a	2.722 ± 0.04 ^b	3.671 ± 0.03 ^c	4.512 ± 0.05 ^d	26	10.035 ± 0.05 ^a	8.935 ± 0.06 ^b	14.770 ± 0.08 ^c	15.616 ± 0.06 ^d
27	2.493 ± 0.06 ^a	2.865 ± 0.02 ^b	3.940 ± 0.04 ^c	4.820 ± 0.09 ^d	27	10.775 ± 0.06 ^a	9.444 ± 0.03 ^b	16.028 ± 0.09 ^c	16.801 ± 0.03 ^d
28	2.614 ± 0.02 ^a	3.012 ± 0.01 ^b	4.225 ± 0.02 ^c	5.141 ± 0.03 ^d	28	11.551 ± 0.04 ^a	9.965 ± 0.04 ^b	17.366 ± 0.05 ^c	18.052 ± 0.02 ^d
29	2.739 ± 0.01 ^a	3.164 ± 0.01 ^b	4.525 ± 0.01 ^c	5.477 ± 0.06 ^d	29	12.363 ± 0.07 ^a	10.498 ± 0.02 ^b	18.790 ± 0.04 ^c	19.373 ± 0.01 ^d
30	2.868 ± 0.07 ^a	3.321 ± 0.07 ^b	4.840 ± 0.06 ^c	5.826 ± 0.05 ^d	30	13.213 ± 0.08 ^a	11.042 ± 0.01 ^b	20.301 ± 0.06 ^c	20.766 ± 0.06 ^d

^aCS Chitosan s, PVA Polyvinyl alcohol

^bResults are presented as means ± SD ($n = 3$)

^cValues with different letters in the same row indicate significant difference ($p \leq 0.05$)

On the other hand, the adsorption of water molecules in PVA films increases the size of cavities as shown by the data obtained in this work. Hodge [47] mentioned that the sorption of water in PVA occurs in three stages; during the initial stage, the water adsorption (less than 8%) takes place. The water enters as individual molecules or vapor state and binds to the hydroxyl groups of PVA through hydrogen bonds. At this point, the adsorbed water molecules do not modify the mean pore radius. In the second stage, the pore size increases significantly until 30% of moisture content, approximately. This increase could be due to the expansion of the interchain distances in the water molecules due to the filling of pores without swelling of the polymer. In the last stage, a decrease in density takes place mainly because of hydrogen bond disruption and swelling of the polymeric matrix. The increase of pore size indicates a larger free volume due to swelling of the polymer [47].

The results suggest that the chemical composition, molecular packing, and swelling of polymers, influence the formation of micro or mesoporous as a function of temperature and moisture content. Pore radio is an important parameter to be considered in rehydration, humectability, and functional properties of polymers intended for food packaging.

Thermodynamic Properties of Films

Integral Enthalpy

Integral enthalpy (ΔH)_{int} indicates the degree of interaction between water molecules and the film. The CS films showed a zone of maximum equilibrium heat of 19 kJ/mol in a range from 0.45 to 0.60 of a_w . The PVA films exhibited 28 kJ/mol at 0.35 of a_w Fig. 2. After this point, a reduction in enthalpy to 5 kJ/mol as the a_w increased was observed. In the case of PVA films, the well-defined peak indicated that a maximum value of energy was reached. Then, strongest water-film interactions took place. Low enthalpies values (less than 60 kJ/mol) are associated with physical adsorption [48]. This behavior could be attributed to a significant reduction of intermolecular attractive forces between sorption sites of films and water molecules as the water activity increases, indicating that the energy used during the adsorption process was equal to the energy used for condensation for free water [49], implying that the water molecules present at high a_w are highly mobile leading to further deterioration reaction. Because of the enthalpy values in which water vapor is being adsorbed, it is assumed that a physisorption phenomenon is taking place in CS and PVA films.

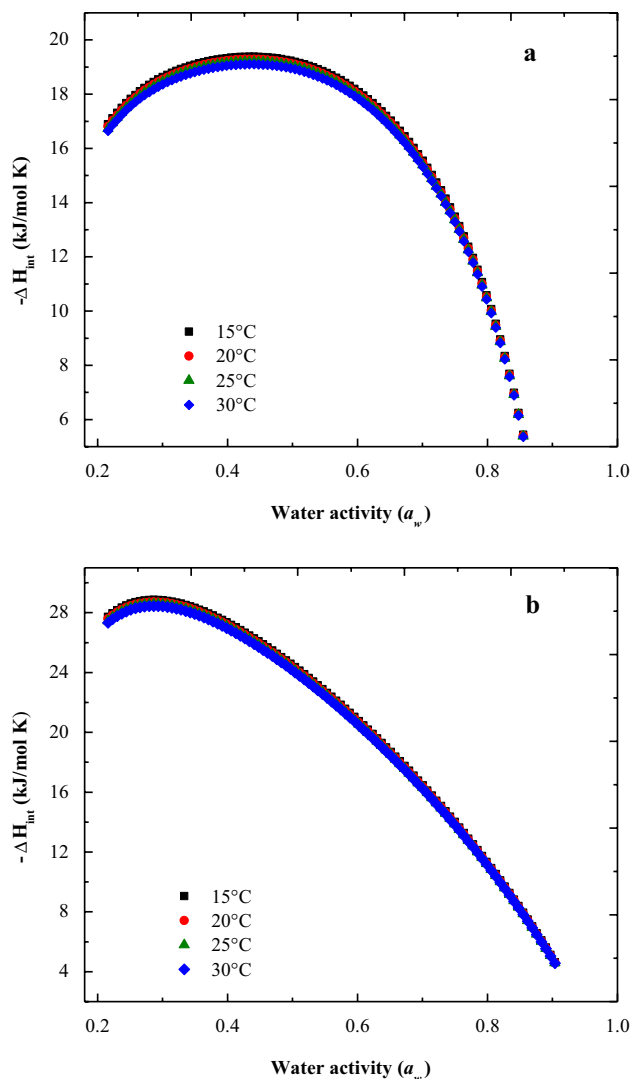


Fig. 2 Integral enthalpy changes of adsorbed water on **a** Chitosan films and **b** PVA films as function of water activity

At the same level of a_w (0.35), the CS films bind water with less energy, but they were able to keep this water (until 0.6 of a_w , approximately) and then, a gradual release of bound water took place. The PVA films reached a maximum level of energy at 0.3 of a_w , and after that, the energy to bind water decreased quickly, resulting in emptying of specific adsorption sites. The low enthalpy values at the low a_w region are a good indication of the degree of occupation of binding sites in the films. Thus, under the same adsorption conditions, the CS and PVA films bind water in a different way. Films from CS can keep the water molecules bound meanwhile PVA films bind water with stronger energy, but they are not able to keep it as the a_w increases. This fact could be attributed to the physical properties and the chemical structure of both polymers. It seems like in the interaction of CS with water not only the hydroxyl groups

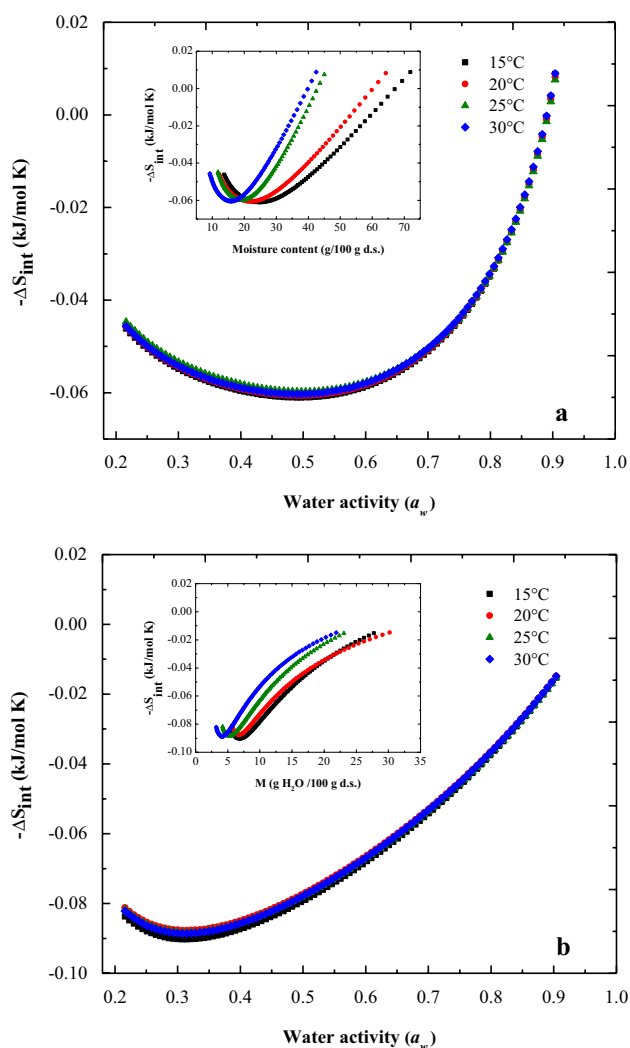


Fig. 3 Integral entropy changes of adsorbed water on **a** Chitosan and **b** PVA films as function of water activity

participate but also the amino group [35]. For PVA-based films, the formation of inter and intramolecular hydrogen bonds between OH groups influence its hydration and determines the interaction with water molecules [16].

Integral Entropy

The integral entropy describes the arrangement of water molecules taking place during the adsorption process [33]. The minimum integral entropy is considered as the maximum stability point [32, 50]. Figure 3 shows the integral entropy of CS and PVA films as a function of a_w at 15 °C, 20 °C, 25 °C, and 30 °C. The integral entropy decreased until reaching a minimum point and then increased as the a_w increased. The decrease in integral entropy indicates a diminution of the water molecules mobility promoting the saturation of binding sites and, consequently, a higher energy is

required for the adsorption process. On the other hand, the increasing of integral entropy implies that water molecules can form multilayers. At high moisture contents, entropy will be approximately the same as liquid water [51].

In the case of CS and PVA films, a zone of minimum entropy was observed Fig. 3, however, minimum a_w values were identified in the data. For CS films, the water activity with the minimum of entropy was allocated around 0.491 corresponding to moisture content of 24.673 %, 21.878 %, 19.082 %, and 15.784 % at 15 °C, 20 °C, 25 °C, and 30 °C, respectively. As the temperature increased, the integral entropy in PVA decreased. The water activity for maximum stability of PVA was around 0.314 corresponding to moisture content of 6.890 %, 6.731 %, 5.258 %, and 4.114 % at 15 °C, 20 °C, 25 °C, and 30 °C, respectively. In both films, the moisture content of maximum stability decreased when the temperature increased; this effect was more noticeable in films based on chitosan. In CS films, the region in which the integral entropy changed little with the moisture content was located at the a_w range between 0.47 and 0.54. Thus, according to the values of minimum integral entropy, CS films may be stored at higher a_w values than the PVA films.

Compensation Enthalpy-Entropy

The compensation theory allows knowing if the water adsorption is driven by enthalpy or entropy mechanism [52]. The isokinetic (T_B) and the harmonic medium temperature (T_{hm}) are parameters used to evaluate it. The isokinetic temperature is an important physical parameter because it represents the temperature at which all reactions are carried out at the same rate [53]. T_B and T_{hm} were calculated for CS and PVA films. The compensation theory applies if T_B is different from the harmonic T_{hm} . The value obtained for T_{hm} was 295.55 K for CS and PVA films. According to the Krug test criteria [28, 54] if the T_B is higher than T_{hm} , the process is controlled by enthalpy. Conversely, if the T_B is lower than T_{hm} , the process is controlled by the entropy.

Figure 4 shows the values of the isokinetic temperature and the harmonic medium temperature for the PVA and CS films. Two lines for each film are shown, indicating adsorption regions, related to low and high values of a_w . The arrows indicate the direction of water adsorption from lowest to highest equilibrium moisture content. T_{B1} and T_{B2} represent the integral isokinetic temperature at low and high a_w values, respectively. From the obtained results, it is assumed that at lower a_w values the adsorption was driven by enthalpy, while at high values of a_w it was controlled by entropy for CS and PVA-based films. These results indicate that the sorption mechanism was driven by the physical structure of the films in the first stage, when the a_w was lower (0.3–0.5 for CS and 0.2–0.3 for PVA) while that at intermediate and high values of a_w (0.5–0.9 for CS and 0.4–0.9 for PVA) the mechanism

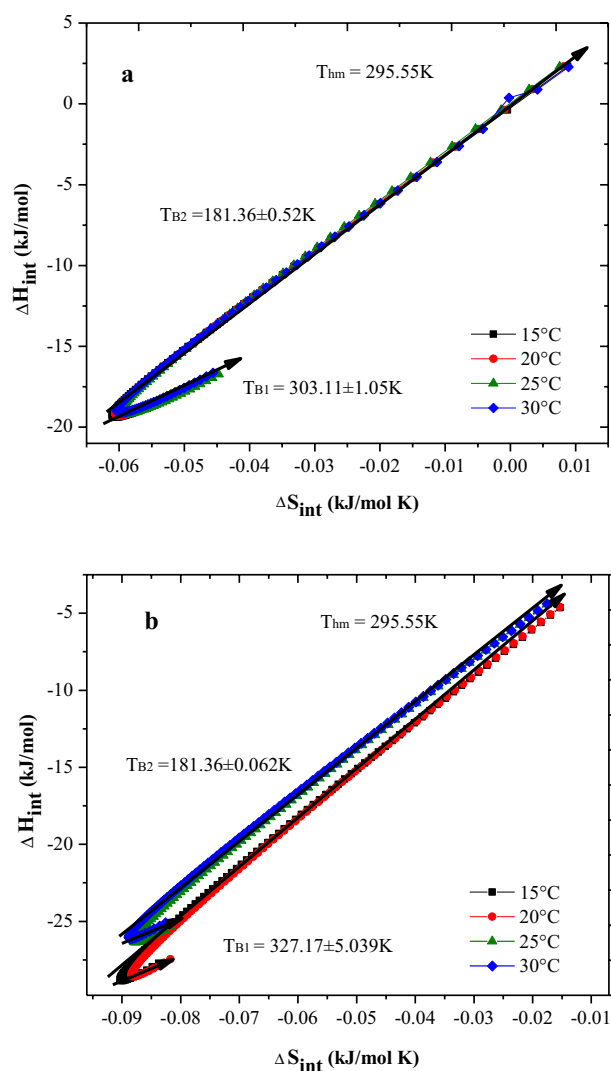


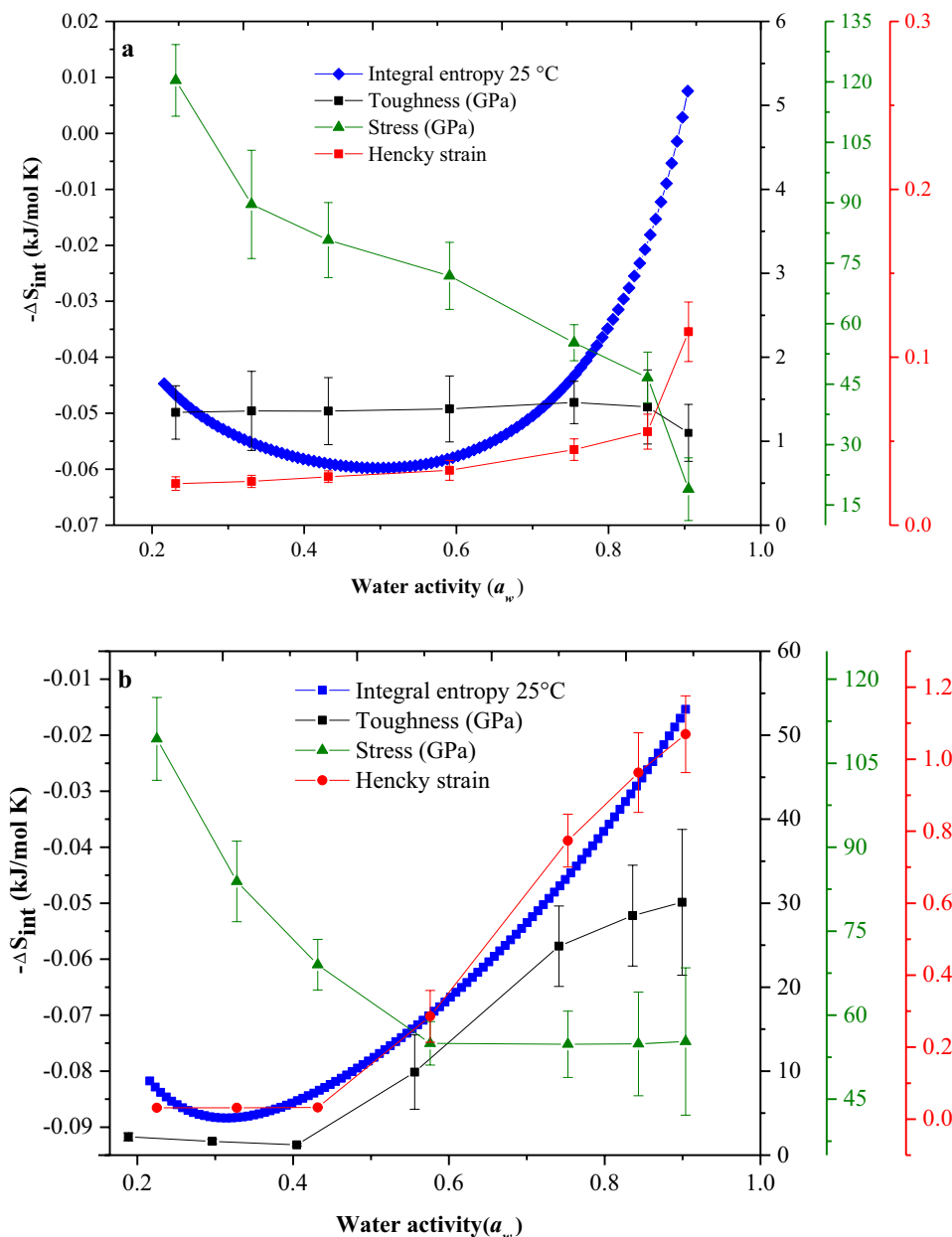
Fig. 4 Compensation theory of **a** Chitosan, **b** PVA

was driven by energetical interactions which depend on the chemical composition of the polymers conforming the films.

Mechanical Properties

The mechanical properties of films showed a strong dependence on a_w . The maximum stress value for CS films was observed at a_w values lower than 0.2; after this, a step-like decrease was displayed, followed by a deeply decrease in 0.75 of a_w Fig. 5a. As the a_w increased in CS films, the stress values decreased up to 19 GPa. It is noticeable that the constant value of toughness was presented in the range where the zone of ΔS_{int} was also found Fig. 5a. HS describes the deformation of the films. From the results, it is possible to observe that in the 0.2–0.4 a_w range, the HS values are low and remained constant Fig. 5a. At 0.45 of a_w , the HS increased slightly, and remained quasi-constant until 0.6 of

Fig. 5 Mechanical properties of **a** Chitosan and **b** PVA films as function of water activity



a_w Fig. 5a. The CS films showed a maximum HS value at 0.9 of a_w . This behavior indicates that a deformation in chitosan films was observed after the ΔS_{int} was achieved (0.47–0.54 of a_w). Previous reports associated the decreasing of tensile strength and the increase in the percent of elongation at break of the polymers with a plasticization process [11, 12].

In the case of PVA films, the lowest and constant values of toughness and HS were observed in the range from 0.1 to 0.45 of a_w Fig. 5b. It is noticeable that in PVA films, the lowest values were observed in the range where the zone of ΔS_{int} was also found. As the a_w increased (>0.45), the values of mechanical properties increased until achieving maximum values at 0.9 of a_w . It is remarkable the higher

value of HS and toughness for PVA films (1.1 GPa and 29.4 GPa, respectively) compared to CS films. This result reveals the greater deformation capacity and breaking strength of PVA-based films.

The stress value of PVA films presented a maximum value (115 GPa) at water activities lower than 0.1. Then, a step-like decrease in stress value was displayed, followed by a deeply decrease in 0.55 of a_w reaching a value of 56 GPa, where it remained constant up to 0.9 of a_w Fig. 5b. Surprisingly, this a_w did not match with ΔS_{int} .

The HS and stress behavior in both films were similar Fig. 5a and b. However, the deformation of CS films is gradual compared with PVA films, but PVA shows higher

deformation. It is probably because chitosan is a more ramified and hydroxylated polymer that could interact easily by electrostatic forces with water molecules. Hencky strain evidenced that at values lower than 0.5 of a_w , the films preserved 80% of its resistance to deformation. On the other hand, the CS films evidenced a greater degree of interaction with water molecules.

The adsorption of water molecules in hydrophilic materials promotes structural changes modifying the mechanical properties [55] because it is a small molecule that can penetrate the structure breaking bonds and leading to fragile materials when the moisture content is low (0.1–10 %) [56]. As hydrophilic polymers, the mechanical properties of CS and PVA films were modified when exposed at different conditions of the relative humidity of equilibrium. This effect was more noticeable at water activities higher than 0.7. Similar behavior has been reported for PVA, CS, alone or blended with other materials as well as films based on other biopolymers [11, 57–60].

The point at which the mechanical properties suddenly decrease could be considered as an indication of excessive hydration. When the hydrophilic materials are excessively hydrated the mechanical properties (toughness, stress, and HS) change drastically. It is corroborated in this work because toughness in both types of film (CS and PVA) drastically changed its values at 0.7 of a_w . Similar results were reported by [11] in the mechanical properties of PVA films. They found a deeply changes in elastic modulus and fracture resistance at $a_w=0.57$.

Conclusions

Moisture adsorption isotherms showed that CS films were more hygroscopic adsorbing two-folds more moisture than PVA films at the highest a_w in all temperatures studied. The moisture content for the minimum of integral entropy recognized as the point of maximum stability decreased as a function of temperature and this behavior was more evident in CS films. The thermodynamic behavior indicates that, under the same adsorption conditions, CS and PVA films bind water in a different way. The compensation theory evidenced that at lower a_w values, the sorption is governed by enthalpy. Hencky strain evidenced that before 0.5 of a_w , the CS and PVA films preserved 80% of its resistance to deformation. Most of the mechanical properties showed constant values at the zone of minimum integral entropy, confirming that the thermodynamic properties could be used to predict the stability of films. The optimal storage conditions of CS and PVA films intended for food packaging application can be defined through the moisture adsorption, thermodynamic properties, and the mechanical properties.

Author Contributions RYAL: Conceptualization; Resources; Methodology; Software; Validation; Investigation; Writing—Original Draft; Writing—Review & Editing; Visualization; Supervision; Project administration. G V: Conceptualization; Resources; Writing—Original Draft; Project administration; Funding acquisition. Validation; Formal analysis. AYGL: Conceptualization; Data Curation; Writing—Original Draft; Writing—Review & Editing; Visualization; Supervision. RVC: Conceptualization; Data Curation; Writing—Original Draft; Writing—Review & Editing; Visualization; Supervision; Validation; Formal analysis. JC: Conceptualization; Data Curation; Writing—Original Draft; Writing—Review & Editing; Visualization; Supervision. Validation; Formal analysis.

Funding This research did not receive any specific grant from funding agencies in the public, commercial, or not-for-profit sectors.

Data Availability The authors declare the transparency of data.

Code Availability Software and programs used in this manuscript have license to be used.

Declarations

Conflict of Interest The authors have no relevant financial or non-financial interests to disclose.

Ethical Approval The authors statement that the manuscript it is original and it has not been submitted elsewhere.

Consent to Participate Not applicable.

Consent for Publication Not applicable.

References

1. Cazon P, Vázquez M, Velazquez G (2018) Cellulose-glycerol-polyvinyl alcohol composite films for food packaging: evaluation of water adsorption, mechanical properties, light-barrier properties and transparency. *Carbohydr Polym* 195(9):432–443. <https://doi.org/10.1016/j.carbpol.2018.04.120>
2. Aider M (2010) Chitosan application for active bio-based films production and potential in the food industry. *LWT-Food Science and Technology* 43(6):837–842. <https://doi.org/10.1016/j.lwt.2010.01.021>
3. Neto CDT, Giacometti JA, Job AE, Ferreira FC, Fonseca JLC, Pereira MR (2005) Thermal analysis of chitosan based networks. *Carbohydr Polym* 62(2):97–103. <https://doi.org/10.1016/j.carbpol.2005.02.022>
4. Ahmadi F, Oveysi Z, Samani SM, Amoozgar Z (2015) Chitosan based hydrogels: characteristics and pharmaceutical applications. *Res Pharm Sci* 10(1):1
5. Dresvyanina EN, Grebennikov SF, Elovhovskii VY, Dobrovolskaya IP, Ivan'kova EM, Yudin VE, Heppe K, Morganti P (2020) Thermodynamics of interaction between water and the composite films based on chitosan and chitin nanofibrils. *Carbohydrate Polym* 245: 116552. <https://doi.org/10.1016/j.carbpol.2020.116552>
6. Koski A, Yim K, Shivkumar SJML (2004) Effect of molecular weight on fibrous PVA produced by electrospinning. *Mater Lett* 58(3–4):493–497

7. Jiang S, Liu S, Feng W (2011) PVA hydrogel properties for biomedical application. *J Mech Behav Biomed Mater* 4(7):1228–1233
8. Deshmukh K, Ahamed MB, Deshmukh RR, Pasha SK, Bhagat PR, Chidambaram K (2017) Biopolymer composites with high dielectric performance: interface engineering. *Biopolymer composites in electronics*. Elsevier p. 27–128.
9. Srinivasa PC, Ramesh MN, Kumar KR, Tharanathan RN (2003) Properties and sorption studies of chitosan–polyvinyl alcohol blend films. *Carbohydr Polym* 53(4):431–438. [https://doi.org/10.1016/S0144-8617\(03\)00105-X](https://doi.org/10.1016/S0144-8617(03)00105-X)
10. Teodorescu M, Bercea M, Morariu S (2019) Biomaterials of PVA and PVP in medical and pharmaceutical applications: perspectives and challenges. *Biotechnol Adv* 37(1):109. <https://doi.org/10.1016/j.biotechadv.2018.11.008>
11. Aguirre-Loredo RY, Rodríguez-Hernández AI, Morales-Sánchez E, Gómez-Aldapa CA, Velazquez G (2016) Effect of equilibrium moisture content on barrier, mechanical and thermal properties of chitosan films. *Food Chem* 196:560–566. <https://doi.org/10.1016/j.foodchem.2015.09.065>
12. Bourbon AI, Pinheiro AC, Cerqueira MA, Rocha CMR, Avides MC, Quintas MAC, Vicente AA (2011) Physico-chemical characterization of chitosan-based edible films incorporating bioactive compounds of different molecular weight. *J Food Eng* 106(2):111–118. <https://doi.org/10.1016/j.jfoodeng.2011.03.024>
13. Cissé M, Montet D, Tapia MS, Loiseau G, Ducamp-Collin MN (2012) Influence of temperature and relative humidity on the immobilized lactoperoxidase system in a functional chitosan film. *Food Hydrocolloids* 28(2):361–366. <https://doi.org/10.1016/j.foodhyd.2012.01.012>
14. Gómez-Aldapa CA, Velazquez G, Gutierrez MC, Rangel-Vargas E, Castro-Rosas J, Aguirre-Loredo RY (2020) Effect of polyvinyl alcohol on the physicochemical properties of biodegradable starch films. *Mater Chem Phys* 239:122027. <https://doi.org/10.1016/j.matchemphys.2019.122027>
15. Rouhi M, Razavi SH, Mousavi SM (2017) Optimization of crosslinked poly(vinyl alcohol) nanocomposite films for mechanical properties. *Mater Sci Eng, C* 71(2):1052–1063. <https://doi.org/10.1016/j.msec.2016.11.135>
16. Satokawa Y, Shikata T (2008) Hydration structure and dynamic behavior of poly (vinyl alcohol)s in aqueous solution. *Macromolecules* 41(8):2908–2913. <https://doi.org/10.1021/ma702793t>
17. McCune TD, Lang KW, Steinberg MP (1981) Water activity determination with the proximity equilibration cell. *J Food Sci* 46(6):1978–1979. <https://doi.org/10.1111/j.1365-2621.1981.tb04542.x>
18. Labuza TP, Kaanane A, Chen JY (1985) Effect of temperature on the moisture sorption isotherms and water activity shift of two dehydrated foods. *J Food Sci* 50(2):385–392. <https://doi.org/10.1111/j.1365-2621.1985.tb13409.x>
19. Cassini AS, Marczak LDF, Noreña CPZ (2006) Water adsorption isotherms of texturized soy protein. *J Food Eng* 77(1):194–199. <https://doi.org/10.1016/j.jfoodeng.2005.05.059>
20. Rosa GS, Moraes MA, Pinto LAA (2010) Moisture sorption properties of chitosan. *LWT Food Sci Technol* 43(3):415–420. <https://doi.org/10.1016/j.lwt.2009.09.003>
21. Sonwane CG, Bhatia SK (2000) Characterization of pore size distributions of mesoporous materials from adsorption isotherms. *J Phys Chem B* 104(39):9099–9190. <https://doi.org/10.1021/jp000907j>
22. Moraes K, Pinto LAA (2012) Desorption isotherms and thermodynamic properties of anchovy in natura and enzymatic modified paste. *J Food Eng* 110(4):507–513. <https://doi.org/10.1016/j.jfoodeng.2012.01.012>
23. Esquerdo VM, Monte M L, de Pinto LA (2019) Microstructures containing nanocapsules of unsaturated fatty acids with biopolymers: characterization and thermodynamic properties. *J Food Eng* 248: 28–35. <https://doi.org/10.1016/j.jfoodeng.2018.12.015>
24. Monte ML, Moreno ML, Senna J, Arrieche LS, Pinto LAA (2018) Moisture sorption isotherms of chitosan-glycerol films: Thermodynamic properties and microstructure. *Food Biosci* 22(February):170–177. <https://doi.org/10.1016/j.fbio.2018.02.004>
25. Othmer DF (1940) Correlating vapor pressure and latent heat data. *Ind Eng Chem* 32:841–856. <https://doi.org/10.1021/ie50366a022>
26. Beristain CI, Diaz R, Garcia HS, Azuara E (1994) Thermodynamic behavior of green whole and decaffeinated coffee beans during adsorption. *Drying Technol* 12:1221–1233. <https://doi.org/10.1080/07373939408960997>
27. Wexler A (1976) Vapor pressure formulation for water in range 0 to 100°C. A revision. *J Res Nat Bureau Standards Sect A Phys Chem* 80:775–785. <https://doi.org/10.6028/jres.080A.071>
28. Krug RR, Hunter WG, Grieger RA (1976) Enthalpy-entropy compensation. 1. Some fundamental statistical problems associated with the analysis of van't Hoff and Arrhenius data. *J Phys Chem* 80:2335–2341. <https://doi.org/10.1021/j100562a006>
29. ASTM (2012) D882–12 Standard test method for tensile properties of thin plastic sheeting. *ASTM Int*, West Conshohocken, PA. <https://doi.org/10.1520/D0882-12>
30. Brunauer S, Emmett PH, Teller E (1938) Adsorption of gases in multimolecular layers. *J Am Chem Soc* 60:301–319. <https://doi.org/10.1021/ja01269a023>
31. Bell LN, Labuza T (2000) Moisture sorption: practical aspects of isotherm measurement and use, 2nd edn. American Association of Cereal Chemists, Inc., St. Paul, USA (ISBN: 1891127187, 9781891127182)
32. Viveros-Contreras R, Téllez-Medina DI, Perea-Flores MJ, Alamilla-Beltrán L, Cornejo-Mazón M, Beristain-Guevara CI, Azuara-Nieto E, Gutiérrez-López GF (2013) Encapsulation of ascorbic acid into calcium alginate matrices through coacervation coupled to freeze-drying. *Revista Mexicana de Ingeniería Química* 12(1): 29–39. <http://rmiq.org/ojs311/index.php/rmiq/article/view/1449>
33. Viganó J, Azuara E, Telis V, Beristain CI, Jiménez M, Telis-Romero J (2012) Role of enthalpy and entropy in moisture sorption behavior of pineapple pulp powder produced by different drying methods. *Thermochim Acta* 528:63–71. <https://doi.org/10.1016/j.tca.2011.11.011>
34. Alpizar-Reyes E, Castaño J, Carrillo-Navas H, Alvarez-Ramírez J, Gallardo-Rivera R, Pérez-Alonso C, Guadarrama-Lezama AY (2018) Thermodynamic sorption analysis and glass transition temperature of faba bean (*Vicia faba* L.) protein. *J Food Sci Technol* 55(3):935–943. <https://doi.org/10.1007/s13197-017-3001-1>
35. McLaughlin CP, Magee TRA (1998) The determination of sorption isotherm and the isosteric heats of sorption for potatoes. *J Food Eng* 35(3):267–280. [https://doi.org/10.1016/S0260-8774\(98\)00025-9](https://doi.org/10.1016/S0260-8774(98)00025-9)
36. Rueda DR, Secall T, Bayer RK (1999) Differences in the interaction of water with starch and chitosan films as revealed by infrared spectroscopy and differential scanning calorimetry. *Carbohydr Polym* 40(1):49–56. [https://doi.org/10.1016/S0144-8617\(99\)00033-8](https://doi.org/10.1016/S0144-8617(99)00033-8)
37. Guadarrama-Lezama AY, Jaramillo-Flores E, Gutiérrez-López GF, Pérez-Alonso C, Dorantes-Álvarez L, Alamilla-Beltrán L (2014) Effects of storage temperature and water activity on the degradation of carotenoids contained in microencapsulated chili extract. *Drying Technol* 32(12):1435–1447. <https://doi.org/10.1080/07373937.2014.900502>
38. Aguirre-Loredo RY, Rodríguez-Hernandez AI, Velazquez G (2017) Modelling the effect of temperature on the water sorption

- isotherms of chitosan films. *Food Sci Technol* 37(1):112–118. <https://doi.org/10.1590/1678-457x.09416>
39. Alpizar-Reyes E, Carrillo-Navas H, Romero-Romero R, Varela-Guerrero V, Alvarez-Ramírez J, Pérez-Alonso C (2017) Thermodynamic sorption properties and glass transition temperature of tamarind seed mucilage (*Tamarindus indica* L.). *Food Bioprod Process* 101:166–176. <https://doi.org/10.1016/j.fbp.2016.11.006>
 40. Pascual-Pineda LA, Alamilla-Beltrán L, Gutiérrez-López GF, Azuara E, Flores-Andrade E (2017) Prediction of storage conditions of dehydrated foods from a water vapor adsorption isotherm. *Revista Mexicana de Ingeniería Química* 16:207–220. <https://doi.org/10.24275/rmiq/Alim817>
 41. Enrione J, Hill S, Mitchell JR, Pedreschi F (2010) Sorption behavior of extruded rice starch in the presence of glycerol. *Water Prop Food Health Pharm Biol Syst ISOPOW* 10:483–489
 42. Martín-Martínez JM (1990) Adsorción física de gases y vapores por carbones. Universidad de Alicante, Secretariado de Publicaciones (ISBN: 84-86809-33-9)
 43. Mucha M, Ludwiczak S (2006) Dynamics of water sorption to nanopores of polymer biomaterials. *Mol Cryst Liq Cryst* 448(1):133–735. <https://doi.org/10.1080/15421400500387882>
 44. Ogawa K, Yui T, Okuyama K (2004) Three D structures of chitosan. *Int J Biol Macromol* 34(1–2):1–8. <https://doi.org/10.1016/j.ijbiomac.2003.11.002>
 45. Rivero S, Damonte L, García MA, Pinotti A (2016) An insight into the role of glycerol in chitosan films. *Food Biophys* 11(2):117–127. <https://doi.org/10.1007/s11483-015-9421-4>
 46. Okuyama K, Noguchi K, Miyazawa T, Yui T, Ogawa K (1997) Molecular and crystal structure of hydrated chitosan. *Macromolecules* 30(19):5849–5855. <https://doi.org/10.1021/ma970509n>
 47. Hodge RM, Bastow TJ, Edward GH, Simon GP, Hill AJ (1996) Free volume and the mechanism of plasticization in water-swollen poly (vinyl alcohol). *Macromolecules* 29(25):8137–8143. <https://doi.org/10.1021/ma951073j>
 48. Smith JM, Van Ness HC, Abbott MM (2005) Introduction to chemical engineering thermodynamics. McGraw-Hill, New York. ISBN 13: 9780071270557.
 49. Xiao Q, Tong Q (2013) Thermodynamic properties of moisture sorption in pullulan–sodium alginate based edible films. *Food Res Int* 54(2):1605–1612. <https://doi.org/10.1016/j.foodres.2013.09.019>
 50. Bonilla E, Azuara E, Beristain CI, Vernon-Carter EJ (2010) Predicting suitable storage conditions for spray-dried microcapsules formed with different biopolymer matrices. *Food Hydrocolloids* 24(6):633–640. <https://doi.org/10.1016/j.foodhyd.2010.02.010>
 51. McMinn WAM, Magee TRA (2003) Thermodynamic of moisture sorption of potato. *J Food Eng* 60(2):157–165. [https://doi.org/10.1016/S0260-8774\(03\)00036-0](https://doi.org/10.1016/S0260-8774(03)00036-0)
 52. Azuara E, Beristain CI (2006) Enthalpic and entropic mechanisms related to water sorption of yogurt. *Drying Technol* 24(11):1501–1507. <https://doi.org/10.1080/07373930600961173>
 53. Gabas AL, Menegalli FC, Telis-Romero J (2000) Water sorption enthalpy-entropy compensation based on isotherms of plum skin and pulp. *J Food Sci* 65(4):680–680. <https://doi.org/10.1111/j.1365-2621.2000.tb16072.x>
 54. Krug RR, Hunter WG, Grieger RA (1976) Enthalpy-entropy compensation. 2-Separation of the chemical from the statistical effect. *J Phys Chem* 80:2341–2351. <https://doi.org/10.1021/j100562a007>
 55. Suppakul P, Chalernsook B, Ratisuthawat B, Prapasitthi S, Munchukangwan N (2013) Empirical modeling of moisture sorption characteristics and mechanical and barrier properties of cassava flour film and their relation to plasticizing–antiplasticizing effects. *LWT-Food Science and Technology* 50(1):290–297. <https://doi.org/10.1016/j.lwt.2012.05.013>
 56. Castaño J, Bouza R, Rodríguez-Llamazares S, Carrasco C, Vinicius R (2012) Processing and characterization of starch-based materials from pehuen seeds (*Araucaria araucana* (Mol) K. Koch). *Carbohydr Polym* 88:299–307. <https://doi.org/10.1016/j.carbpol.2011.12.008>
 57. Cazon P, Velazquez G, Vazquez M (2020) Regenerated cellulose films combined with glycerol and polyvinyl alcohol: effect of moisture content on the physical properties. *Food Hydrocolloids* 103(6):105657. <https://doi.org/10.1016/j.foodhyd.2020.105657>
 58. Cazon P, Vazquez M, Velazquez G (2020) Regenerated cellulose films with chitosan and polyvinyl alcohol: effect of the moisture content on the barrier, mechanical and optical properties. *Carbohydr Polym* 236(5):116031. <https://doi.org/10.1016/j.carbpol.2020.116031>
 59. Cazon P, Velazquez G, Vazquez M (2020) Environmentally friendly films combining bacterial cellulose, chitosan and polyvinyl alcohol: effect of water activity on barrier, mechanical and optical properties. *Biomacromol* 21(2):753–760. <https://doi.org/10.1021/acs.biomac.9b01457>
 60. Liu L, Liang H, Zhang J, Zhang P, Xu Q, Lu Q, Zhang C (2018) Poly(Vinyl Alcohol)/chitosan composites: physically transient materials for sustainable and transient bioelectronics. *J Clean Prod* 195(10):786–795. <https://doi.org/10.1016/j.jclepro.2018.05.216>

Publisher's Note Springer Nature remains neutral with regard to jurisdictional claims in published maps and institutional affiliations.